Development 135, 1725-1734 (2008) doi:10.1242/dev.014043

Deafness in mice lacking the T-box transcription factor Tbx18 in otic fibrocytes

Mark-Oliver Trowe[1], Hannes Maier[2], Michaela Schweizer[3] and Andreas Kispert[1,*]

In the cochlea, fibrocytes play important physiological roles, including the maintenance of the ionic composition of the endolymph. Human deafness upon fibrocyte alterations witnesses their crucial role for hearing. We demonstrate that differentiation of otic fibrocytes requires the T-box transcription factor gene *Tbx18*. *Tbx18* expression during inner ear development is restricted to the sub-region of otic mesenchyme that is fated to differentiate into fibrocytes. We rescued the somitic defect that underlies the perinatal lethality of *Tbx18*-mutant mice by a transgenic approach, and measured auditory brainstem responses. Adult *Tbx18*-deficient mice showed profound deafness and a complete disruption of the endocochlear potential that is essential for the transduction of sound by sensory hair cells. The differentiation of otic fibrocytes of the spiral ligament was severely compromised. Tissue architecture of the stria vascularis of the lateral wall was disrupted, exhibiting an almost complete absence of the basal cell layer, and a reduction and changes of intermediate and marginal cells, respectively. Stria vascularis defects resulted from the failure of *Tbx18*-mutant otic fibrocytes to generate the basal cell layer by a mesenchymal-epithelial transition. Defects in otic fibrocyte differentiation may be subordinate to a primary role of *Tbx18* in early compartmentalization of the otic mesenchyme, as lineage restriction and boundary formation between otic fibrocytes and the surrounding otic capsule were severely affected in the mutant. Our study sheds light on the genetic control of patterning and differentiation of the otic mesenchyme, uncovers distinct steps of stria vascularis formation and illuminates the importance of non-epithelially-derived otic cell types for normal hearing and the etiology of deafness.

KEY WORDS: Inner ear, Otic fibrocytes, Otic mesenchyme, Stria vascularis, Deafness, Mouse

INTRODUCTION

The cochlea of the inner ear is a sensory apparatus that converts the mechanical stimulation of sound into electrical activity. A crucial factor in sound transduction, and thus hearing, is the maintenance of the ionic homeostasis of the endolymph, the extracellular fluid of the cochlear duct. The importance of fibrocyte integrity in this process has become apparent by pathological changes caused by inherited disorders or environmental stress. Genetic ablation of certain fibrocyte-expressed genes is known to cause deafness (Minowa et al., 1999; Teubner et al., 2003; Boettger et al., 2003; Delprat et al., 2005), and noise-induced, as well as age-related, hearing deficits are initiated by changes in fibrocyte physiology (Hequembourg and Liberman, 2001; Hirose and Liberman, 2003).

Otic fibrocytes represent a heterogeneous population of cells with special structural and molecular adaptations according to their location and physiological properties (Spicer and Schulte, 1991). Fibrocytes are found in the spiral limbus at the proximal site of the cochlea, and in the spiral ligament in the cochlear lateral wall, where five subgroups can be distinguished (see Fig. 1A). Type I fibrocytes underlie the stria vascularis, a specialized non-sensory epithelial thickening of the lateral wall, type II fibrocytes are situated under the spiral prominence, type III fibrocytes line, as a thin layer, the otic capsule, type IV fibrocytes are located lateral to the basilar membrane and anchor it to the lateral wall (Henson and Henson, 1988), and type V fibrocytes reside above the stria vascularis. Fibrocytes of subtypes I, II and V are highly interconnected, and form a mesenchymal gap junction network. This and an independent epithelial network couple non-sensory supporting cells of the Organ of Corti with basal and intermediate cells of the stria vascularis (for a review, see Kikuchi et al., 2000). Basal cells form a multi-layered epithelial barrier that separates the extracellular spaces of the stria vascularis and the spiral ligament. Neural crest-derived intermediate cells form a discontinuous layer between basal cells and marginal cells that constitutes an epithelial barrier facing the endolymph in the cochlear duct (see Fig. 1B for a scheme of the cellular structure of the stria) (for reviews, see Forge and Wright, 2002; Raphael and Altschuler, 2003). The mesenchymal gap junction network plays a central role in ionic homeostasis. In fact, recycling of K^+-ions through this network is pivotal for cochlear physiology. Strial marginal cells actively transport K^+-ions into the endolymph to maintain a very high concentration in this compartment. A voltage gradient between the negative potential inside the sensory hair cells and the positive endocochlear potential (EP) in the endolymph, together with the concentration gradient in the same direction, drives the influx of K^+-ions through apical mechano-sensitive channels and, thus causes the depolarization of hair cells. After secretion by hair cells and re-uptake by supporting cells, K^+-ions are thought to travel through the epithelial and mesenchymal gap junction networks back to the stria vascularis (for reviews, see Kikuchi et al., 2000; Wangemann, 2002).

Despite the importance of otic fibrocytes for the physiology and pathology of hearing, little insight has been gained into the genetic circuits regulating fibrocyte development. Mice mutant for the transcription factor gene *Pou3f4* (also known as *Brn4*) show ultrastructural alterations in fibrocyte morphology and exhibit a reduced EP and profound deafness (Minowa et al., 1999; Phippard et al., 1999). In mice mutant for otospiralin (*Otos*), a gene encoding a small extracellular matrix (ECM) protein of unknown function,

[1]Institut für Molekularbiologie, Medizinische Hochschule Hannover, Carl-Neuberg-Strasse 1, 30625 Hannover, Germany. [2]HNO Klinik, Universitätsklinikum Eppendorf, Universität Hamburg, Martinistrasse 52, 20246 Hamburg, Germany. [3]Zentrum für Molekulare Neurobiologie Hamburg (ZMNH), Universität Hamburg, Martinistrasse 52, 20246 Hamburg, Germany.

*Author for correspondence (e-mail: kispert.andreas@mh-hannover.de)

Accepted 28 February 2008

fibrocytes type II and IV are degenerated (Delprat et al., 2005). Similar to *Pou3f4*, the precise role of *Otos* in fibrocyte differentiation is unknown.

This report defines a critical role in the development of otic fibrocytes for Tbx18, a member of the evolutionary conserved family of T-box transcription factors (Naiche et al., 2005). Mice carrying a null allele of *Tbx18* die shortly after birth with severe malformations of the vertebral column and the rib cage (Bussen et al., 2004), prominent hydroureternephrosis (Airik et al., 2006) and defective caval veins (Christoffels et al., 2006), defects that have been traced to crucial functions of the gene in somite patterning, differentiation of the ureteric mesenchyme and myocardialization of caval veins, respectively. Here, we uncover an additional requirement for *Tbx18* in the development of the inner ear. We show that adult *Tbx18*-deficient mice with rescued lethality display profound deafness, and we analyze the electro-physiological, histological and molecular changes that underlie this phenotype. We correlate the expression of *Tbx18* in otic mesenchyme with defects in fibrocyte composition and stria vascularis integrity, and characterize the etiology of the defects.

MATERIALS AND METHODS

Mice

Generation of $Tbx18^{lacZ}$ and *msd::Tbx18* transgenic mouse lines was described previously (Bussen et al., 2004; Airik et al., 2006). The generation of a GFP allele of *Tbx18* ($Tbx18^{GFP}$) that was interchangeably used with the *lacZ* allele will be described elsewhere. All mouse lines were maintained on an NMRI outbred background. Embryos for *Tbx18* expression analysis were derived from matings of NMRI wild-type mice. $Tbx18^{-/-}$ embryos were obtained from matings of *Tbx18* heterozygotes. Mice compound heterozygous for a *Tbx18* mutant allele and the *msd::Tbx18* transgene were mated to derive viable adult double homozygous mice. Wild-type or heterozygous littermates were used as controls for mutant embryos and mice. Genomic DNA prepared from yolk sac or tail biopsies was used for genotyping by PCR. For timed pregnancies, vaginal plugs were checked in the morning after mating, noon was taken as embryonic day (E) 0.5. Embryos were dissected in phosphate-buffered saline (PBS) and fixed in 4% paraformaldehyde (PFA) in PBS.

Histological analyses

Embryos were embedded in paraffin wax and sectioned to 5 μm. Inner ears were dissected from adult temporal bones and fixed in Bouin's fixative for 48 hours, decalcified in 0.5 M EDTA/PBS for 48 hours, dehydrated, paraffin wax embedded and sectioned to 5 μm. Sections were stained with Hematoxylin and Eosin or Picro-Sirius Red (F3BA, Sigma-Aldrich, USA). Histochemistry for β-galactosidase activity was carried out on cryosections as described (Lobe et al., 1999).

Ultrastructural analysis

For the preparation of ultra-thin sections, cochleae from anaesthetized 3-week-old *Tbx18KO* and control animals (one each) were quickly removed and perfused through the round window with 3% glutaraldehyde in cacodylat buffer, and then left in the fixative overnight. Fixed cochleae were decalcified in 10% EDTA (pH 7.3) at 4°C for 3 days, cut in two, post-fixed in 2% osmium tetroxide for 30 minutes, dehydrated in a graded series of ethanol solutions and embedded in Epon. Ultra-thin sections (60 nm) were stained with uranyl acetate and lead citrate and examined with a Zeiss 902 electron microscope.

Immunohistochemistry and immunofluorescence

Adult inner ears were fixed in 4% PFA overnight, decalcified in 0.5 M EDTA/PBS, pH 8, for 48 hours, embedded in paraffin wax and cut to 5 μm. Alternatively, decalcified cochleae were immersed in 30% sucrose/PBS for 12 hours, embedded in tissue-freezing medium (Leica, Germany), and cryosectioned to 5 μm. For the detection of antigens, the following primary antibodies and dilutions were used. Polyclonal rabbit antisera against Aqp1 (1:200, Alomone Labs), Barttin (1:100, gift from Friedhelm Hildebrandt) (Birkenhager et al., 2001), E-cadherin (1:200, gift from Rolf Kemler) (Vestweber and Kemler, 1984), Glut1 (1:200, Dianova), Kcc3 (1:500, gift from Thomas Jentsch) (Boettger et al., 2003), Kcnq1 (1:250, gift from Thomas Jentsch) (Dedek and Waldegger, 2001), Kir4.1 (1:200, Alomone Labs), laminin (1:100, Sigma) and otospiralin (1:250, gift from Christian Hamel) (Delprat et al., 2002); polyclonal guinea pig-anti-connexin26 (1:200, gift from Johanna Brandner) (Brandner et al., 2004); and monoclonal mouse antibodies against Atp1a1 (Na-K-ATPase subunit 1a, clone a6F, 1:500, developed by Douglas M. Farmbrough and obtained from the Developmental Studies Hybridoma Bank, University of Iowa) and Cldn11 (clone 37E3, 1:500, gift from Alexander Gow) (Gow et al., 2004). Fluorophore-coupled secondary antibodies were purchased from Dianova, Germany (Rhodamine-Red-X-conjugated donkey-anti-mouse, Rhodamine-Red-X-conjugated goat-anti-rabbit, Cy3-conjugated goat-anti-guinea pig), Invitrogen, USA (Alexa-488 conjugated donkey-anti-rabbit) and Santa Cruz Biotechnology, USA (FITC-conjugated goat-anti-mouse, FITC-conjugated goat-anti-rabbit), and used at a dilution of 1:200. Non-fluorescent staining was performed using kits from Vector Laboratories (Mouse-on-Mouse peroxidase kit, Vectastain ABC peroxidase kit (Rabbit IgG), DAB substrate kit). Labeling with the primary antibody was performed at 4°C overnight after antigen retrieval (2 mM EDTA in 0.01 M Tris-HCl, pH9, at 80°C, 1 hour) and blocking in 3% BSA, 3% normal goat serum for 30 minutes in PBST. For monoclonal mouse antibodies an additional IgG blocking step was performed using the Mouse-on-Mouse Kit (Vector Laboratories).

In situ hybridization analysis

In situ hybridization analysis on 10 μm sagittal sections of E18.5 heads was performed following a standard procedure with digoxigenin-labeled antisense riboprobes (Moorman et al., 2001). Details of probes used are available upon request.

Documentation

Sections were photographed using a Leica DM5000 microscope with a Leica DFC300FX digital camera. Laser scanning microscopy was performed using a Leica TCS SP2 microscope. All images were processed in Adobe Photoshop CS.

Hearing assessment

Auditory brainstem responses were measured as described previously (Boettger et al., 2002). In cases where no auditory response could be recorded at the highest obtainable level of 137 dB peak equivalent sound pressure level, the hearing threshold was set to this value for statistical analysis. Measurement of the endocochlear potential (EP) followed published procedures (Boettger et al., 2003).

RESULTS

Tbx18 is expressed in prospective otic fibrocytes

In order to assess the spatial distribution of *Tbx18* transcripts during inner ear development, we performed an in situ hybridization analysis of sagittal sections of mouse heads at different embryonic stages. Since we detected *Tbx18* expression in otic mesenchyme, we compared on adjacent sections expression of the chondrogenic marker gene *Sox9* (Lefebvre and de Crombrugghe, 1998) and expression of *Pou3f4*, whose expression marks the entire early periotic mesenchyme (Phippard et al., 1998) (Fig. 2). Inner ear expression of *Tbx18* was first detected in ventral aspects of the mesenchyme surrounding the otic vesicle at embryonic day (E) 11.5 (Fig. 2A). *Tbx18* expression partially overlapped *Sox9* and *Pou3f4* expression, whose domains, however, were clearly more expanded at this stage (Fig. 2B,C). Expression of *Tbx18* and *Sox9* started to become mutually exclusive at E12.5. *Tbx18* expression was confined to the inner zone of the periotic mesenchyme in the whole inner ear, including the future cochlea and the vestibular portion (Fig. 2D,G; data not shown), whereas *Sox9* expression was restricted to the outer zone, which undergoes chondrogenic differentiation to form the otic capsule from E13.5 onwards (Fig. 2E,H). Expression

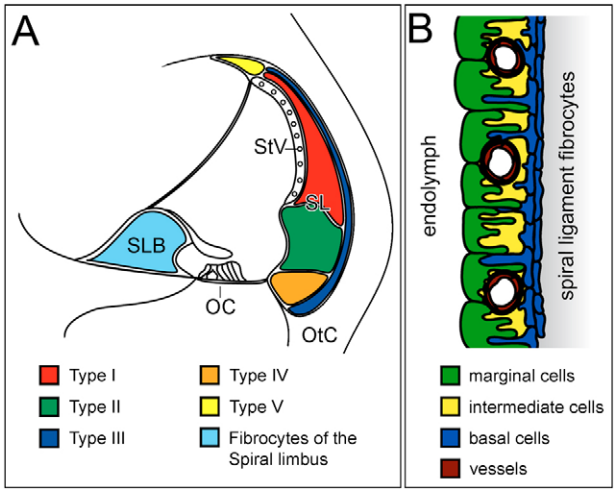

Fig. 1. Diversity of fibrocytes in the cochlea and structure of the stria vascularis. (**A**) Illustration of the distribution of subtypes of otic fibrocytes on a midmodiolar cochlea section. Subtypes are as indicated in the figure. Based on location, cell morphology and marker gene expression, five major types of fibrocytes can be distinguished in the spiral ligament. (**B**) Scheme of the cellular structure of the stria vascularis. Cell types are as indicated in the figure. Stria vascularis integrity relies on a three-layered tissue architecture of marginal, intermediate and basal cells that enclose a dense capillary network. The formation of long cell processes by all three cell types and a high degree of interdigitation characterizes strial architecture. OC, Organ of Corti; OtC, otic capsule; SL, spiral ligament; SLB, spiral limbus; StV, stria vascularis.

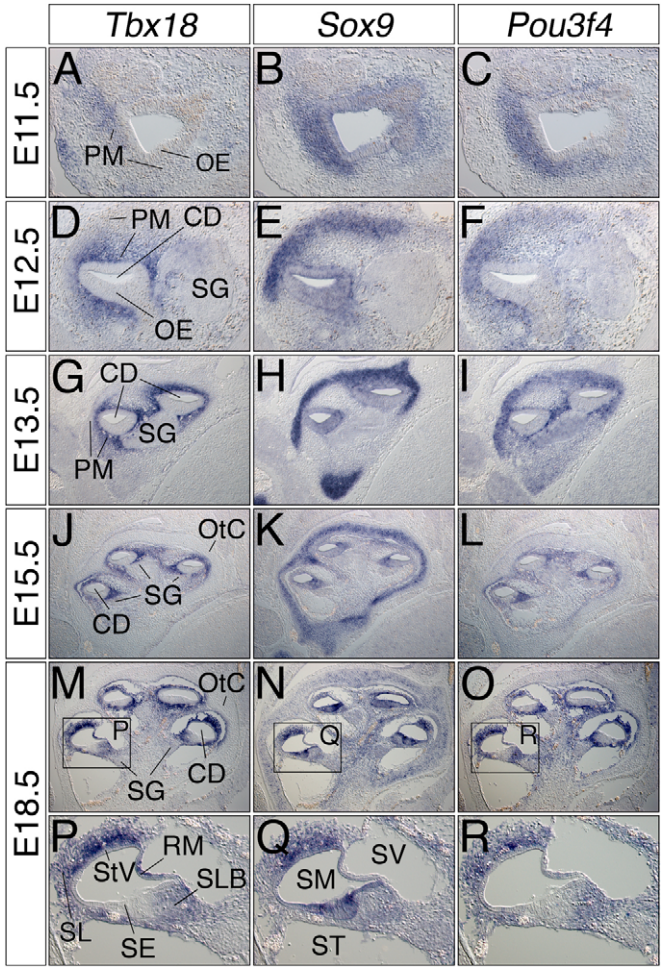

Fig. 2. *Tbx18* expression indicates early compartmentalization of otic mesenchyme. (**A-R**) Comparative analysis of *Tbx18, Sox9* and *Pou3f4* expression during cochlea development by RNA in situ hybridization on adjacent sagittal sections of wild-type heads. Probes and developmental stages are as indicated in the figure. (A,D,G,J,M,P) *Tbx18* expression is confined to the inner zone of periotic mesenchyme representing prospective otic fibrocytes during all developmental stages. (B,E,H,K,N,Q) Mesenchymal *Sox9* expression is found in regions of high cell condensation, like the early periotic mesenchyme, the prospective otic capsule, the condensing spiral limbus and the condensing mesenchyme underlying the future stria vascularis. (C,F,I,L,O,R) Developmental expression of *Pou3f4* in the inner ear is initially pan-mesenchymal but becomes restricted to prospective otic fibrocytes after E13.5. CD, cochlear duct; OE, otic epithelium; OtC, otic capsule; PM, periotic mesenchyme; RM, Reissner's membrane; SE, sensory epithelium; SG, spiral ganglion; SL, spiral ligament; SLB, spiral limbus; SM, scala media; ST, scala tympani; StV, stria vascularis; SV, scala vestibuli.

of *Pou3f4* was found throughout the periotic mesenchyme, overlapping *Tbx18* and *Sox9* expression until E13.5 (Fig. 2F,I). From E15.5 until E18.5, *Tbx18* expression was restricted to prospective otic fibrocytes of the spiral limbus and the spiral ligament (Fig. 2J,M). Expression was upregulated in condensing mesenchyme underlying the stria vascularis at E18.5 (Fig. 2P). *Sox9* expression was downregulated in the otic capsule after E15.5, but was found in condensing mesenchymal cells at E18.5 (Fig. 2K,N,Q). *Pou3f4* and *Tbx18* expression domains overlapped from E15.5 to E18.5 (Fig. 2L,O,R). *Tbx18* expression was not detected at postnatal day (P) 21, when inner ear development is completed (data not shown). Hence, *Tbx18* expression was restricted to an inner zone of otic mesenchyme fated to differentiate into otic fibrocytes, throughout inner ear development.

Tbx18 is required for hearing

Mice homozygous for a null allele of *Tbx18* die shortly after birth due to severe malformation of the vertebral column. This phenotype was traced to a requirement for *Tbx18* in the anterior-posterior polarization of somites (Bussen et al., 2004). To evaluate the functional significance of *Tbx18* expression in otic mesenchyme, we sought to overcome the perinatal lethality of *Tbx18*-deficient mice by re-introducing somitic expression of *Tbx18*. We used transgenic *msd::Tbx18* mice that express *Tbx18* throughout the presomitic and somitic mesoderm, but not in the inner ear (Bussen et al., 2004) (see Fig. S1 in the supplementary material), to generate mice compound mutant for a *Tbx18* loss-of-function allele and the *msd::Tbx18* transgene. Mice double homozygous for *Tbx18* and *msd::Tbx18* were born in the expected Mendelian ratio. They were smaller than their littermates and exhibited a general impaired mobility, explainable by skeletal defects. They survived for 3-4 months before they died from hydronephrotic lesions. Although vestibular function seemed normal in these mice, acoustic Preyer reflexes were absent, indicating a severe hearing deficit. We examined auditory function by measuring auditory brainstem responses (ABRs) to clicks, with an upper frequency limit of 5.5 kHz, shortly after the onset of hearing (at P14) in three- and twelve-week-old *Tbx18/Tbx18,msd::Tbx18/msd::Tbx18* (*Tbx18KO*) mice and *Tbx18/+,msd::Tbx18/+* (control) littermates. *Tbx18KO* mice showed an ABR with clicks of about 130 dB peak equivalent sound

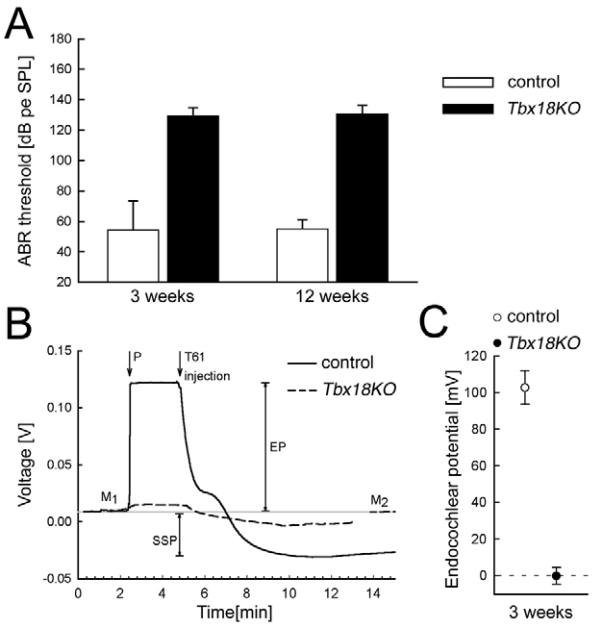

Fig. 3. Loss of *Tbx18* causes deafness. (**A-C**) Analysis of hearing by ABR (A) and EP (B,C) measurements of *Tbx18KO* and control mice. (A) ABR thresholds are significantly increased in *Tbx18KO* mice at three weeks (129.3±5.3 dB pe SPL, *n*=15) and 12 weeks (130.5±5.8 dB pe SPL, *n*=10) compared with control animals of the same age (3 weeks: 54.2±19.2 dB pe SPL, *n*=18; 12 weeks, 54.9±6.4 dB pe SPL, *n*=8). (B) Registration of the EP in *Tbx18KO* (dashed line) and control mice (solid line) at P21. After taking the reference DC potential in the fluid meniscus overlying the stria vascularis (M_1), the recording electrode was moved forward. Upon penetration of the stria vascularis (P), the EP was measured in the scala media for at least 2 minutes before the animal was sacrificed by the injection of a barbiturate (T61). Within several minutes of the insult, the EP decreased to a negative steady-state-potential (SSP) – reaching a minimum after 8-12 minutes. In contrast to the EP, which is given by the steady state of active and passive ionic current components, the SSP reflects only the passive part of the ionic conductivities, as long as ion concentrations are minimally altered after active transport has come to a halt. As a control for baseline shifts, the reference DC potential was measured after the experiment (M_2) to verify its constancy over the entire time. (C) Disruption of the EP and SSP in *Tbx18KO* mice at three weeks of age (control: EP=102.9±9.1 mV, SSP=–26.4±9.9 mV, *n*=10; *Tbx18KO*: EP=1.3±3.1 mV, SSP=–3.8±3.9 mV, *n*=10). The difference in EP and SSP is significant (*P*<0.001, Mann-Whitney Rank Sum Test); bars indicate standard deviation.

pressure level (pe SPL) at both time-points; the average increase was >75 dB above the hearing threshold of control animals (Fig. 3A). Thus, *Tbx18KO* mice had a pronounced hearing loss at three weeks of age.

As the excitability of hair cells depends on the magnitude of the EP, a reduced EP would explain the elevation of the ABR threshold in *Tbx18KO* mice. Evaluation of the EP in *Tbx18KO* mice at P21 revealed a complete breakdown of the EP (Fig. 3B,C). Together, these results demonstrate that loss of *Tbx18* expression in otic mesenchyme leads to an abnormal otic physiology and a severely compromised auditory function.

Lateral wall hypoplasia in *Tbx18KO* mice

Histological analysis of three-week-old *Tbx18KO* inner ears did not reveal any obvious changes in cochlear shape, but an overall reduction in size was apparent (Fig. 4B), and the spiral ganglion was not completely surrounded by bone tissue of the modiolus (Fig. 4D). The lateral wall, including stria vascularis and otic fibrocytes, of the spiral ligament was severely hypoplastic, the spiral prominence was variably reduced (white arrow in Fig. 4F,J). Suprastrial (type V) fibrocytes were absent, and type IV fibrocytes lateral to the basilar membrane were partially replaced by bone tissue (arrow and arrowhead in Fig. 4F,J). The number of cells underlying the stria vascularis was drastically diminished and the spiral prominence was different from that of controls, indicating additional defects in type I and II fibrocytes (Fig. 4D,F). The stria vascularis of *Tbx18KO* mice was variably reduced, with a thin stripe of flat marginal cells extending into Reissner's membrane (Fig. 4J). Ultrastructural analysis of the stria vascularis architecture at 3 weeks of age revealed presence of marginal, intermediate and basal cells, but their densely packed membranous infoldings were severely reduced in *Tbx18KO* animals (Fig. 4L). Phenotypic changes in the lateral wall gradually increased in severity towards the basal end of the cochlea duct. The Organ of Corti appeared normal at this stage (Fig. 4H). At 12 weeks of age, defects of the lateral wall had increased in severity. The stria vascularis was flattened to a thin layer of simple squamous epithelial cells (see Fig. S2 in the supplementary material).

Hence, the cyto-architecture of the lateral wall, including the fibrocytes of the spiral ligament and the epithelial barrier cells of the stria vascularis, is severely affected by the loss of *Tbx18* function in development.

Improper differentiation of otic fibrocytes in *Tbx18KO* mice

Expression of *Tbx18* in otic fibrocytes, disruption of the EP and histological changes in the lateral wall of *Tbx18*-deficient mice suggested a role for *Tbx18* in the differentiation of otic fibrocytes. To explore this possibility in more detail, we analyzed the distribution of proteins defining fibrocyte subtypes by immunohistochemistry.

Otospiralin (Otos), an ECM protein of unknown function, is expressed in all otic fibrocytes (Delprat et al., 2002). In *Tbx18KO* mice, Otos was present throughout the spiral ligament, albeit with decreased expression, particularly in the region (of type IV fibrocytes) beneath the basilar membrane (arrow in Fig. 5B). The gap junction protein connexin 26 (Cx26; also known as Gjb2 – Mouse Genome Informatics) marks type I fibrocytes that underlie the stria vascularis (Xia et al., 1999). Cx26 staining was absent in *Tbx18KO* spiral ligament fibrocytes (Fig. 5D). Expression of Atp1a1, the alpha1 polypeptide of the Na^+/K^+-transporting ATPase, is confined to marginal cells of the stria vascularis and to type II, IV and V fibrocytes of the spiral ligament (Xia et al., 1999). In *Tbx18KO* mice, the Atp1a1 expression domain was unchanged but the level of expression in spiral ligament fibrocytes appeared reduced (Fig. 5F). Aquaporin 1 (Aqp1) expression, which is normally restricted to bone lining fibrocytes type III (Li and Verkman, 2001) (arrowheads in Fig. 5G), was lost in the mutant (Fig. 5H). Kcc3 (also known as Slc12a6 – Mouse Genome Informatics) represents a potassium-chloride co-transporter whose expression is found in type I, III and V fibrocytes (Boettger et al., 2003). In the mutant, expression of Kcc3 at strongly reduced levels was homogenous in the spiral ligament (Fig. 5J). Together, histological and immunohistochemical analyses revealed that terminal differentiation of fibrocytes into clearly distinct subpopulations was severely disturbed in the spiral ligament of *Tbx18KO* mice (Fig. 5K).

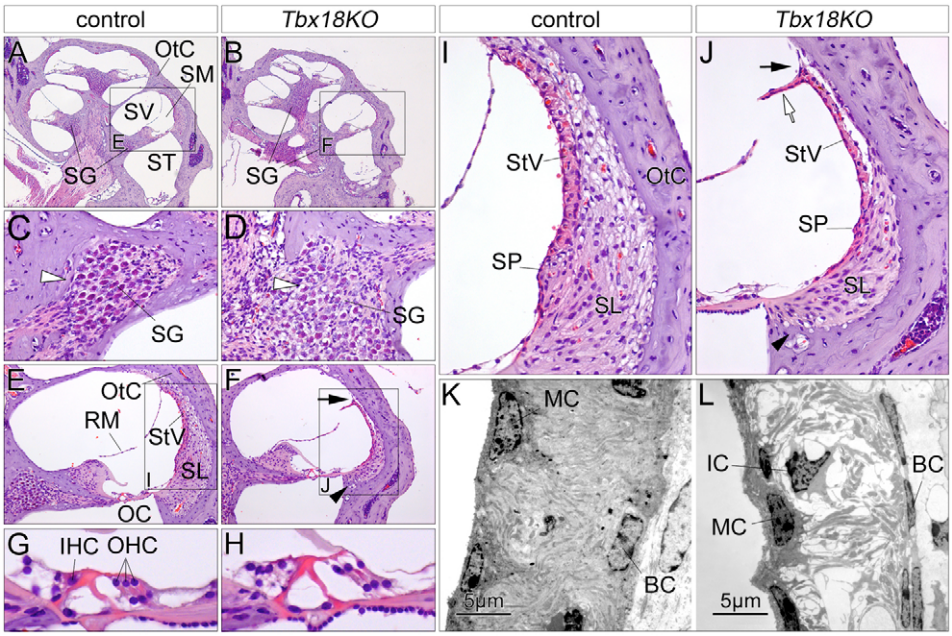

Fig. 4. Histological and ultrastructural defects in the *Tbx18KO* cochlea. Hematoxylin and Eosin staining (**A-J**) of midmodiolar sections of the inner ear and ultastructural analysis of the stria vascularis (**K**,**L**) of control and *Tbx18KO* mice at P21. Black rectangles highlight regions of higher magnification. (A,B) *Tbx18KO* cochleae are normal in shape but reduced in size. (C,D) Higher magnification of the medial region reveals improper encapsulation of the ganglion by bone tissue in *Tbx18KO* mice (white arrowheads). (E,F) Higher magnification of the basal turn reveals hypoplasia of the lateral wall in *Tbx18KO* mice. Arrow and arrowhead in F indicate the loss of suprastrial and type IV fibrocytes, respectively. (G,H) Magnified view of the Organ of Corti does not reveal any obvious phenotypic changes in *Tbx18KO* mice (I,J). Magnification of the lateral wall shows stria vascularis malformations and defects in otic fibrocytes in *Tbx18KO* mice. White arrow in J indicates extension of the marginal cells into Reissner's membrane (RM). (K,L) Ultrastructural analysis of the stria vascularis in the basal coil uncovers the presence of large gaps between the cellular processes of strial cells. BC, basal cells; IC, intermediate cells; MC, marginal cells; OC, Organ of Corti; SP, spiral prominence; for further abbreviations, see Fig. 2.

Loss of basal cells in the stria vascularis of *Tbx18KO* mice

To evaluate the histological changes in the *Tbx18KO* stria vascularis more carefully, we analyzed the localization of marker proteins by immunofluorescence. The potassium channel Kcnq1 is confined to the apical surface of strial marginal cells, whereas the chloride channel subunit Barttin is localized baso-laterally (Estevez et al., 2001). Subcellular localization of Kcnq1 and Barttin was unchanged in *Tbx18KO* mice (Fig. 6B,D), suggesting the presence of marginal cells with normal apicobasal polarity. However, the area of Barttin staining was reduced and exhibited an irregular shape, possibly indicating an improper formation of baso-lateral projections (inset in Fig. 6D). Expression of Kir4.1 (also known as Kcnj10 – Mouse Genome Informatics), an inwardly-rectifying potassium channel of intermediate cells (Ando and Takeuchi, 1999), was reduced in the *Tbx18KO* stria vascularis (Fig. 6F), indicating that the differentiation of intermediate cells, including the formation of membranous infoldings (inset in Fig. 6F) was severely affected. The glucose transporter Glut1 (also known as Slc2a1 – Mouse Genome Informatics) exhibits strong expression in basal and endothelial cells of the stria vascularis (Ito et al., 1993). In the mutant, Glut1 expression was found only in endothelial cells of the few remaining strial vessels (Fig. 6H). The absence of expression of the basal cell-specific protein claudin 11 (Cldn11) (Gow et al., 2004; Kitajiri et al., 2004) in *Tbx18KO* mice (Fig. 6J) confirmed the dramatic reduction of the basal cell layer.

Extensive elongation and interdigitation of strial cells relies on the controlled degradation of the basal lamina underlying the marginal cell layer around birth (Sagara et al., 1995; Kikuchi and Hilding, 1966). In addition to the basal lamina of strial vessels, laminin staining detected the presence of a basal lamina underlying marginal cells in *Tbx18KO* mice (Fig. 6L), which is in agreement with the observed reduction of baso-lateral surface projections of marginal cells. Thus, the cellular architecture of the stria vascularis in *Tbx18KO* is severely disturbed, with a massive decrease of basal cell number, and a vast reduction of membraneous projections of intermediate and marginal cells (Fig. 6M).

Loss of mesenchymal condensations underneath the stria vascularis in *Tbx18*$^{-/-}$ spiral ligaments

The occurrence of strial defects upon loss of *Tbx18* in otic mesenchyme suggested a cellular or trophic contribution of the otic mesenchyme to strial development. To distinguish these possibilities, we analyzed *Tbx18*$^{-/-}$ inner ears at E18.5, when stria vascularis maturation is initiated (Kiernan et al., 2002; Xia et al., 1999). Histological examination revealed condensation of mesenchymal cells underneath the forming stria in the wild type, whereas in *Tbx18*$^{-/-}$ mice cells underneath the stria remained loosely organized at this stage (arrow in Fig. 7B). During our studies, we established that these mesenchymal condensates are characterized by the expression of *Sox9*, E-cadherin (also known as *Cdh1* – Mouse Genome Informatics) and *Cx26* in the wild type (Fig. 7C,E,G). Expression of all three genes was lost in the *Tbx18*-deficient spiral ligament, although the epithelial expression domains of these genes appeared unaffected (Fig. 7D,F,H).

Further markers were used to assess cytodifferentiation of the stria vascularis. Expression of *Bsnd*, which encodes Barttin, in prospective marginal cells (Birkenhager et al., 2001) was detected

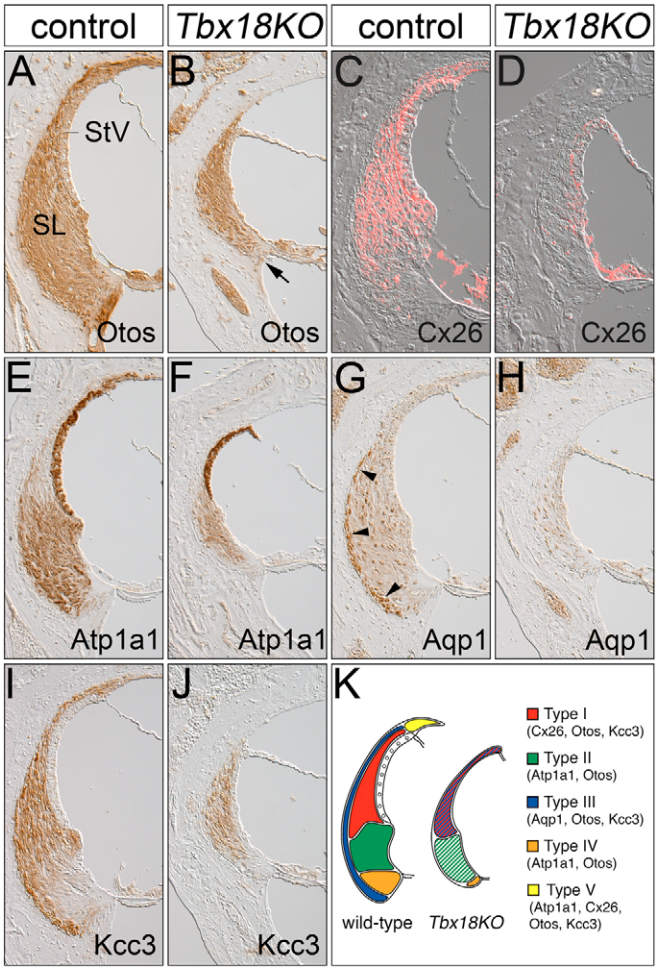

Fig. 5. Differentiation of otic fibrocytes is disturbed in *Tbx18KO* mice. (**A-J**) Localization of otic fibrocyte markers by immunohistochemistry (A,B,E-J) and immunofluorescence (C,D) on midmodiolar sections of cochleae of control and *Tbx18KO* mice at P21. Figures show the lateral wall in the basal turn. Antibodies against proteins specific for fibrocyte subtypes were used as indicated in the figure. Arrow in B marks the loss of strong Otos expression in the region of type IV fibrocytes. (C,D) Overlay of immunofluorescence and differential interference contrast microscopy. Arrowheads in G mark expression in type III fibrocytes. (**K**) Schematic summary of expression domains and fibrocyte subtype distribution in wild-type and *Tbx18KO* cochleae. For abbreviations, see Fig. 2.

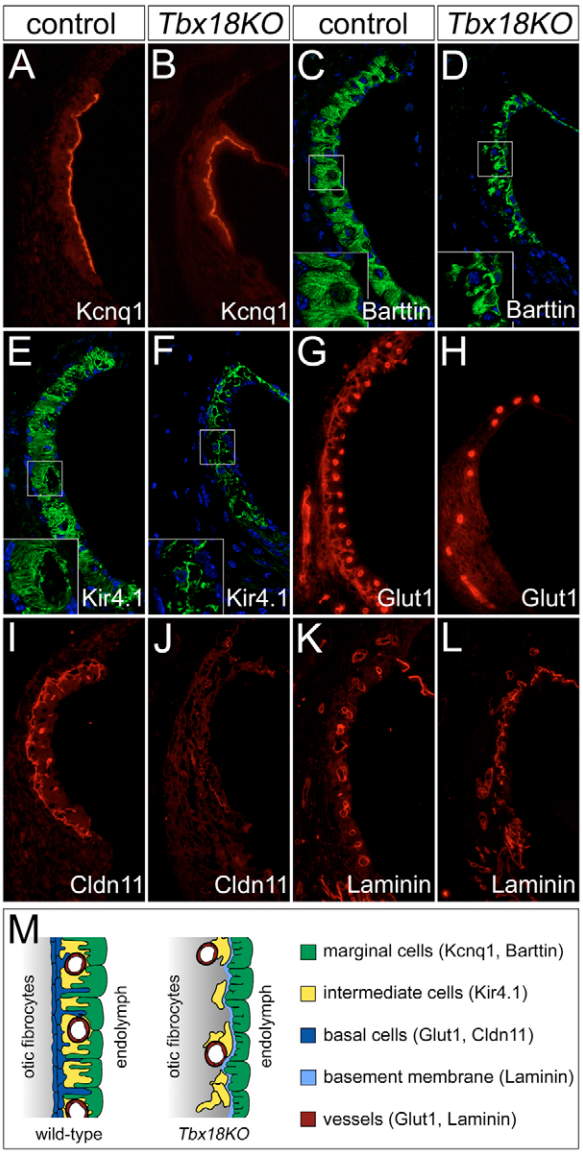

Fig. 6. Defects in the stria vascularis of *Tbx18KO* mice. (**A-L**) Detection of strial proteins by immunofluorescence on midmodiolar sections of cochleae of control and *Tbx18KO* mice at P21. Figures show the stria vascularis in the basal turn. Antibodies against proteins of marginal, intermediate and basal cells, as well as of basement membrane components, were used as indicated in the figure. (C-F) Immunofluorescence on DAPI-counterstained sections detected by laser scanning microscopy. Insets show higher magnifications of the stria vascularis at regions indicated by rectangles in the figures, and reveal the disturbed formation of cellular processes by marginal cells (C,D) and intermediate cells (E,F). (**M**) Schematic summary of expression domains and model of the stria vascularis of wild-type and *Tbx18KO* mice.

in the mutant, suggesting proper temporal regulation of marginal cell differentiation (Fig. 7J). *Dct* (also known as *Trp2*) is a marker for prospective intermediate cells (Steel et al., 1992). *Dct* expression in the mutant was indistinguishable from in the wild type, demonstrating normal homing of future intermediate cells (Fig. 7L). We did not detect changes in the BrdU incorporation of cells of the spiral ligament at E18.5 and E12.5 (n=3 each, data not shown), which suggests that proliferation defects are not a causative agent.

Together, these results suggest that loss of *Tbx18* primarily affects the development of the mesenchymal portion of the cochlea, including the cytodifferentiation of otic fibrocytes. Defects of the stria vascularis may originate from the failure of mesenchymal cells to condense and undergo an epithelial transition to form basal cells.

Disturbed boundary formation between the otic capsule and otic fibrocytes

Tbx18 expression shows an early restriction to the inner ring of otic mesenchyme that will give rise to otic fibrocytes. We wondered whether the observed defects in otic fibrocyte differentiation might be caused, or at least be affected, by a mis-patterning of the otic mesenchyme, indicating an early role for Tbx18 in compartmentalization of this tissue. Improper radial patterning of

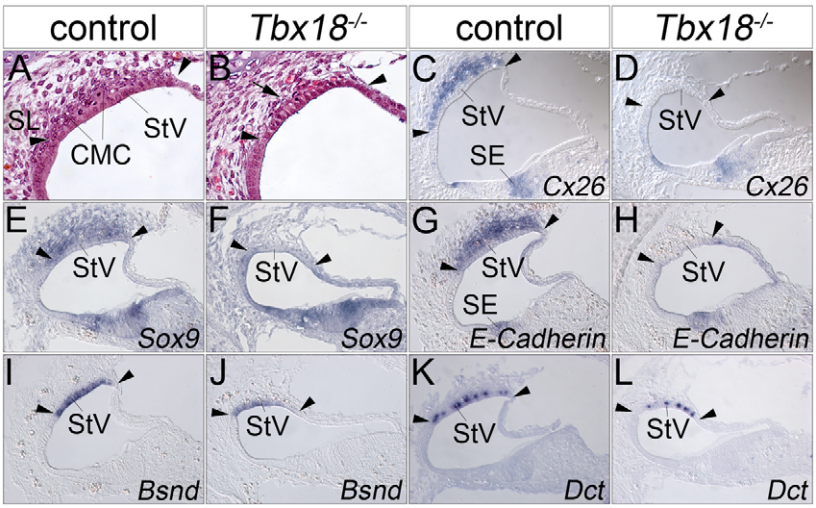

Fig. 7. Developmental manifestation of the stria vascularis phenotype of *Tbx18*$^{-/-}$ mice. Analyses of histology by Hematoxylin and Eosin staining (**A**,**B**) and of marker gene expression by RNA in situ hybridization (**C-L**) on sagittal sections of E18.5 cochleae. Figures show the basal coil (C-L) and the stria vascularis region (A,B). Arrowheads mark the lateral extension of the stria vascularis. *Tbx18*$^{-/-}$ cochleae show normal differentiation of intermediate and marginal cell precursors of the forming stria vascularis, but lack the mesenchymal cell condensation preceding basal cell formation (arrow in B). Probes were used as indicated in the figure. For abbreviations, see Fig. 2.

the otic mesenchyme should reflect in misallocation of cells to the inner and outer compartment, i.e. to otic fibrocytes and the otic capsule, and/or in improper boundary formation. Histological analysis of E18.5 inner ears revealed a local thickening of the otic capsule adjacent to the spiral ligament of *Tbx18*$^{-/-}$ mice (arrow in Fig. 8E), and an altered appearance of otic fibrocyte precursors in the spiral ligament of the basal coil (Fig. 8E). Fibrocytes appeared highly condensed with a preferential parallel orientation to the border of the otic capsule. Collagen staining with Picro-Sirius Red showed a distinct boundary between the fiber systems of the bony otic capsule and the spiral ligament in the wild type at this stage (arrowhead in Fig. 8B). By contrast, in *Tbx18*$^{-/-}$ mice, the collagen fiber network appeared to be continuous between the two regions (Fig. 8F). Following the indications of severe histological changes at the interface between otic capsule and otic fibrocytes, we analyzed expression of periostin (*Postn*), a gene expressed in certain types of fibrous connective tissue, such as the bone-lining periosteum (Horiuchi et al., 1999). *Postn* expression was restricted to cells lining the outer border of the otic capsule and to a small domain in the proximobasal part of the spiral ligament in the wild type at E18.5 (Fig. 8C). In *Tbx18*$^{-/-}$ inner ears, *Postn* was expressed in a distal to proximal gradient throughout the spiral ligament (Fig. 8G). By contrast, expression of *Coch*, which we found to be restricted to a proximal region of the otic mesenchyme underlying the epithelium of the lateral wall in the wild type at this stage (Fig. 8D), was absent in the mutant (Fig. 8H). Expression of *Pou3f4* and *Otos*, which was found throughout the otic mesenchyme in the wild type, was unchanged in *Tbx18*$^{-/-}$ mice at E18.5 (data not shown). Together, these findings suggest that in the *Tbx18*$^{-/-}$ inner ear, the outer compartment of the otic capsule has expanded at the expense of the inner compartment. Mesenchymal cells of the inner compartment have acquired some basal characteristics of otic fibrocytes, but seem to differentiate into periosteum-like connective tissue rather than into distinct fibrocyte subtypes.

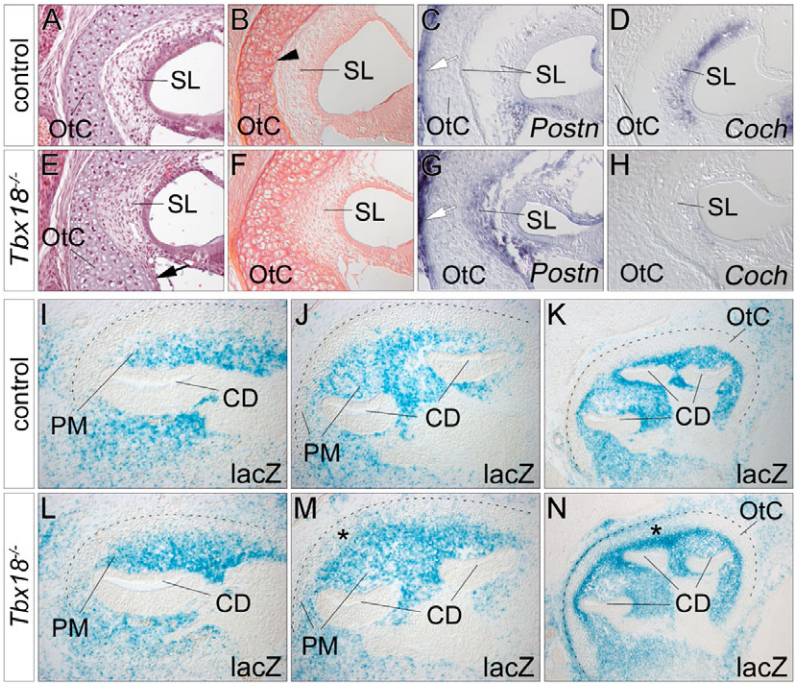

Fig. 8. Disturbed boundary formation between the otic capsule and otic fibrocytes in *Tbx18*$^{-/-}$ mice. (**A-H**) Analyses of histology by Hematoxylin/Eosin (A,E) and Picro-Sirius Red collagen staining (B,F), and of marker gene expression by RNA in situ hybridization (C,D,G,H) on sagittal sections of E18.5 cochleae. Figures show the spiral ligament of the basal coil. Genotypes and probes used are as indicated in the figure. (**I-N**) Analyses of β-galactosidase reporter activity by X-Gal staining on sagittal sections of *Tbx18*^{lacZ}/*Tbx18*^{GFP} and *Tbx18*^{lacZ}/+ (control) mice at E12.5 (I,L), E13.5 (J,M) and E14.5 (K,N). (A,E) HE staining reveals a local expansion of the otic capsule in the basal coil (arrow in E) and altered fibrocyte appearance in the spiral ligament of the mutant (E). (B,F) Collagen staining reveals disturbed boundary formation between spiral ligament fibrocytes and the otic capsule in the *Tbx18*$^{-/-}$ mice. Arrowhead in B marks the compartment boundary in the control. (C,D,G,H) Spiral ligament fibrocytes show ectopic *Postn* (G) and a severe reduction of *Coch* (H) expression in the mutant. White arrow in C,G marks *Postn* expression lining the outer border of the otic capsule. (I-N) β-Galactosidase activity assay detects (former) *Tbx18*-expressing cells in the outer compartment of the periotic mesenchyme (asterisk in M) and the otic capsule (asterisk in N). Dashed lines mark the outer boundary of the periotic mesenchyme and the otic capsule. For abbreviations, see Fig. 2.

We next wished to determine more directly how and when compartmentalization of the otic mesenchyme is affected in the *Tbx18*$^{-/-}$ inner ear. Ideally such an analysis would rely on a genetic fate labeling system that traces the descendants of the inner and outer mesenchymal compartment during development. Presently, such tools that would, for example, be based on *Tbx18* and *Sox9* alleles with inducible cre activity are not available. To circumvent this restriction, we employed β-galactosidase activity from the *Tbx18*^{lacZ} allele for short-time lineage tracing, to follow the fate of *Tbx18*-expressing cells in early inner ear development (Fig. 8I-N). In the heterozygous control (*Tbx18*$^{lacZ/+}$), β-galactosidase activity was restricted to the inner ring of the otic mesenchyme from E12.5 to E14.5, suggesting that compartmentalization of prospective otic fibrocytes occurs as early as E12.5 during development (Fig. 8I-K). By contrast, in *Tbx18* mutant mice with normalized β-galactosidase activity from the *Tbx18*^{lacZ}/*Tbx18*^{GFP} genotype, the β-galactosidase-positive area expanded into the outer ring of condensing mesenchymal cells at E13.5 (Fig. 8M) and reached the outer lining of the cartilagenous otic capsule at E14.5 (Fig. 8N). Hence, cells that normally express *Tbx18* are no longer restricted to the inner compartment of the otic mesenchyme.

DISCUSSION

The establishment and maintenance of the EP as an essential prerequisite for normal hearing depends on the structural and functional integrity of the fibrocyte network of the lateral wall and the stria vascularis. This study shows that the T-box transcription factor gene *Tbx18* is necessary for the proper maintenance of compartment boundaries in the periotic mesenchyme and the differentiation of fibrocyte subtypes from a common precursor population, and provides evidence that basal cell formation is a crucial step of stria vascularis formation that relies on proper fibrocyte integrity.

Tbx18 is necessary for otic fibrocyte differentiation

To our knowledge, *Tbx18* is the earliest molecular marker that shows radially restricted expression in the periotic mesenchyme, demonstrating that molecular subdivision into an inner and outer compartment occurs shortly after mesenchymal aggregation around the otic vesicle. Although we did not formally address the fate of the *Tbx18*-positive otic mesenchyme by genetic lineage tracing experiments, it is likely that *Tbx18* expression from at least E12.5 onwards marks prospective otic fibrocytes. Evidence derives from the mutually exclusive expression domains of *Tbx18* and the chondrogenic marker gene *Sox9*, which in turn becomes quickly restricted to the outer ring of mesenchyme destined to form the otic capsule. In addition, short-time lineage tracing experiments with a *lacZ* reporter in the *Tbx18* locus revealed an early restriction of β-galactosidase activity to the inner compartment of mesenchymal cells.

The spatial restriction of *Tbx18* expression in the developing inner ear is compatible with a role of this transcriptional regulator either in patterning of the periotic mesenchyme in capsule versus fibrocyte compartments, or in specification/differentiation of otic fibrocytes. Dramatic changes in subtype composition of lateral wall fibrocytes in the *Tbx18*-deficient inner ear support a function of *Tbx18* in fibrocyte differentiation. However, for several reasons, we suggest that defects in fibrocyte differentiation are subordinate to a primary requirement of *Tbx18* in patterning or compartmentalization of the otic mesenchyme. First, loss of type I, III and V, and reduction of type IV fibrocytes shows that populations residing in close proximity to the bony capsule are predominantly affected by the loss of *Tbx18*, although the expression of *Tbx18* appears homogenous. More importantly, failure to restrict cells that normally express *Tbx18* to the inner compartment in the mutant after E12.5, local loss of a distinct capsule-fibrocyte boundary at E18.5 coupled with histological alterations of fibrocytes, ectopic expression of *Postn*, and an absence of *Cx26* and *Coch* expression at E18.5 indicate a disturbance of radial patterning of the periotic mesenchyme and a failure to maintain the boundary between mesenchymal compartments destined to give rise to otic capsule and otic fibrocytes. The acquisition of a fate of periosteum-like connective tissue may hamper further differentiation of fibrocytes into the different subtypes.

The failure to restrict cells that normally express *Tbx18* to the inner compartment of the otic mesenchyme may have one of several molecular explanations. First, *Tbx18*$^{-/-}$ cells no longer recognize a repulsive signal emanating from the outer mesenchymal compartment to restrict their migration or intermingling with these cells. Second, *Tbx18*-mutant cells have lost selective adhesiveness. Alternatively, the loss of an inhibitory signal from the *Tbx18*-mutant cells leads to ectopic induction of *Tbx18* in the outer ring of mesenchymal cells. Notably, *Tbx18* has also been implicated in the maintenance of compartment boundaries in somites and in the ureteric mesenchyme. In *Tbx18*$^{-/-}$ somites, posterior somite characteristics expand anteriorly (Bussen et al., 2004), whereas in the metanephric field ureteric mesenchymal cells fail to coalesce onto the ureteric epithelium (Airik et al., 2006). It remains to be explored whether these phenotypes can be rationalized by the disruption of a common molecular program.

To date, a requirement for the proper differentiation of otic fibrocytes has only been demonstrated for *Pou3f4* (Minowa et al., 1999; Phippard et al., 1999). Similar to *Pou3f4*$^{-/-}$ mice, differentiation of fibrocytes is severely compromised in *Tbx18*-deficient mice. However, reduction but not loss of *Pou3f4* expression and more severe phenotypic changes in *Tbx18*$^{-/-}$ animals suggests that there is not a simple epistatic relationship between the two transcription factor genes. More likely, the two genes act in parallel genetic circuits regulating patterning and differentiation of otic mesenchyme.

Requirement for *Tbx18* in fibrocyte differentiation reveals multiple steps in stria vascularis formation

Despite the pivotal role of the stria vascularis in auditory function, little is known about the developmental processes and the underlying molecular pathways involved in its formation. Our study provides molecular evidence that the basal cell layer of the stria vascularis forms by aggregation from, and subsequent mesenchymal-epithelial transition (MET) of, adjacent otic fibrocytes.

Evidence is provided by the co-regulation of *Sox9*, *Cx26* and E-cadherin in condensing mesenchymal cells beneath the stria vascularis. *Sox9*, a gene encoding an HMG-type transcription factor, has been implicated in the regulation of mesenchymal cell condensation in various contexts (Bi et al., 2001; Akiyama et al., 2004), thereby supporting a similar role in this setting. A direct regulation of *Sox9* by Tbx18 is possible. However, it is more likely that the loss of *Sox9* expression is secondary to a prior differentiation defect of the otic mesenchyme. Intriguingly, *Cx26* expression in this domain precedes the onset of K^+-cycling through the gap junction network of the spiral ligament (Sadanaga et al., 1995; Yamasaki et al., 2000). Hence, the expression of *Cx26* might indicate a role in

compartmentalization of cells by gap junction-mediated cell-cell communication (for a review, see Levin, 2007) (see also Ackert et al., 2001). Finally, E-cadherin expression has been implicated in a variety of tissue remodeling processes. The forced expression of E-cadherin in fibroblasts is sufficient to drive them into epithelial cells, whereas the loss of E-cadherin in epithelial cells has been linked to mesenchymal transitions (for a review, see Thiery and Sleeman, 2006) (see also Vanderburg and Hay, 1996). The absence of E-cadherin expression in condensing mesenchymal cells beneath the stria vascularis in the *Tbx18*$^{-/-}$ inner ear strongly supports a functional role of E-cadherin in MET as a prerequisite for basal cell layer formation.

The almost complete loss of basal cells in *Tbx18*$^{-/-}$ mice offered the opportunity to study the role of these cells for marginal and intermediate cell differentiation and maturation. Intermediate cell projections were reduced in the *Tbx18*$^{-/-}$ stria vascularis at three weeks of age, although precursor cells were established normally at E18.5. This favors the idea that expansion, maintenance and/or differentiation of intermediate cells depends on the presence of an intact basal cell layer. Marginal cells showed a mature phenotype with the formation of basolateral processes and expression of the Na^+/K^+-ATPase-α1-isoform (Erichsen et al., 1996). The collapse of Reissner's membrane that has been reported for certain mutants with severely impaired endolymphatic K^+-secretion was not apparent in *Tbx18*$^{-/-}$ mice, suggesting that marginal cells became functional (Delpire et al., 1999; Vetter et al., 1996). We noted, however, that the extension of basolateral processes of marginal cells and interdigitation with intermediate cells was severely compromised, showing that parts of the differentiation program of marginal cells depend on basal and intermediate cells. We propose that basal cell-mediated degradation of the basal lamina is a prerequisite for these processes to occur.

Tbx18 and deafness

The measurement of ABRs revealed profound deafness in *Tbx18*-deficient mice. At three weeks of age, i.e. shortly after the onset of hearing, the EP was completely abolished. Several of our findings suggest that the defect of otic fibrocyte differentiation in *Tbx18KO* mice structurally and functionally interferes with the establishment of a normal EP, both at the level of its strial generation and with the recycling of K^+-ions by the mesenchymal gap junction network.

First, it has recently been demonstrated that expression of the potassium inwardly-rectifying channel Kir4.1 in strial intermediate cells is required for EP generation in the mouse (Marcus et al., 2002). Second, functional integrity of the basal cell layer of the stria vascularis is necessary to establish a distinct intrastrial compartment that, in turn, is required for generation of the EP. Previous studies using *Cldn11* mutant mice showed that loss of the tight junction barrier in basal cells causes a strong decrease of the EP (Gow et al., 2004; Kitajiri et al., 2004). Third, fibrocytes of the spiral ligament have been implicated in the uptake and transport of perilymphatic K^+-ions (for a review, see Kikuchi et al., 2000). Fourth, mice mutant for connexin 30, which exhibits overlapping cochlear expression and forms heteromeric gap junction channels with connexin 26, do not establish a normal EP, illustrating the importance of the spiral ligament gap junction network (Forge et al., 2003; Teubner et al., 2003). Hence, the lack of Kir4.1-positive intermediate cells and the almost complete absence of Cldn11-expressing basal cells in the stria vascularis, the failure in terminal fibrocyte differentiation and the absence of Cx26 expression in the spiral ligament collectively explain the complete abrogation of the EP in *Tbx18*-deficient mice.

In conclusion, we have shown that lack of the T-box transcription factor Tbx18 in otic mesenchyme leads to changes in the compartmentalization and differentiation of otic fibrocytes, and to subsequent defects in stria vascularis formation. Cooperatively, these defects result in a failure to generate a normal EP, dramatically demonstrating the importance of the mesenchymal cells of the lateral wall for auditory function.

We thank Johanna Brandner, Lorraine Everett, Andrew Forge, Alexander Gow, Christian Hamel, Hiroshi Hibino, Thomas Jentsch, Rolf Kemler, Tetsuo Noda, William J. Pavan and Nahid Robertson for reagents, and Rannar Airik, Henner Farin and Achim Gossler for discussion and critical reading of the manuscript. The monoclonal mouse antibodies against Atp1a1 (Na-K-ATPase subunit 1a, clone a6F, developed by Douglas M. Farmbrough were obtained from the Developmental Studies Hybridoma Bank maintained by the University of Iowa. This work was supported by a grant from the German Research Council (DFG KI728/2) to A.K.

Supplementary material

Supplementary material for this article is available at
http://dev.biologists.org/cgi/content/full/135/9/1725/DC1

References

Ackert, C. L., Gittens, J. E., O'Brien, M. J., Eppig, J. J. and Kidder, G. M. (2001). Intercellular communication via connexin43 gap junctions is required for ovarian folliculogenesis in the mouse. *Dev. Biol.* **233**, 258-270.

Airik, R., Bussen, M., Singh, M. K., Petry, M. and Kispert, A. (2006). Tbx18 regulates the development of the ureteral mesenchyme. *J. Clin. Invest.* **116**, 663-674.

Akiyama, H., Chaboissier, M. C., Behringer, R. R., Rowitch, D. H., Schedl, A., Epstein, J. A. and de Crombrugghe, B. (2004). Essential role of Sox9 in the pathway that controls formation of cardiac valves and septa. *Proc. Natl. Acad. Sci. USA* **101**, 6502-6507.

Ando, M. and Takeuchi, S. (1999). Immunological identification of an inward rectifier K+ channel (Kir4.1) in the intermediate cell (melanocyte) of the cochlear stria vascularis of gerbils and rats. *Cell Tissue Res.* **298**, 179-183.

Bi, W., Huang, W., Whitworth, D. J., Deng, J. M., Zhang, Z., Behringer, R. R. and de Crombrugghe, B. (2001). Haploinsufficiency of Sox9 results in defective cartilage primordia and premature skeletal mineralization. *Proc. Natl. Acad. Sci. USA* **98**, 6698-6703.

Birkenhager, R., Otto, E., Schurmann, M. J., Vollmer, M., Ruf, E. M., Maier-Lutz, I., Beekmann, F., Fekete, A., Omran, H., Feldmann, D. et al. (2001). Mutation of BSND causes Bartter syndrome with sensorineural deafness and kidney failure. *Nat. Genet.* **29**, 310-314.

Boettger, T., Hubner, C. A., Maier, H., Rust, M. B., Beck, F. X. and Jentsch, T. J. (2002). Deafness and renal tubular acidosis in mice lacking the K-Cl co-transporter Kcc4. *Nature* **416**, 874-878.

Boettger, T., Rust, M. B., Maier, H., Seidenbecher, T., Schweizer, M., Keating, D. J., Faulhaber, J., Ehmke, H., Pfeffer, C., Scheel, O. et al. (2003). Loss of K-Cl co-transporter KCC3 causes deafness, neurodegeneration and reduced seizure threshold. *EMBO J.* **22**, 5422-5434.

Brandner, J. M., Houdek, P., Husing, B., Kaiser, C. and Moll, I. (2004). Connexins 26, 30, and 43: differences among spontaneous, chronic, and accelerated human wound healing. *J. Invest. Dermatol.* **122**, 1310-1320.

Bussen, M., Petry, M., Schuster-Gossler, K., Leitges, M., Gossler, A. and Kispert, A. (2004). The T-box transcription factor Tbx18 maintains the separation of anterior and posterior somite compartments. *Genes Dev.* **18**, 1209-1221.

Christoffels, V. M., Mommersteeg, M. T., Trowe, M. O., Prall, O. W., de Gier-de Vries, C., Soufan, A. T., Bussen, M., Schuster-Gossler, K., Harvey, R. P., Moorman, A. F. and Kispert, A. (2006). Formation of the venous pole of the heart from an Nkx2-5-negative precursor population requires Tbx18. *Circ. Res.* **98**, 1555-1563.

Dedek, K. and Waldegger, S. (2001). Colocalization of KCNQ1/KCNE channel subunits in the mouse gastrointestinal tract. *Pflugers Arch.* **442**, 896-902.

Delpire, E., Lu, J., England, R., Dull, C. and Thorne, T. (1999). Deafness and imbalance associated with inactivation of the secretory Na-K-2Cl co-transporter. *Nat. Genet.* **22**, 192-195.

Delprat, B., Boulanger, A., Wang, J., Beaudoin, V., Guitton, M. J., Venteo, S., Dechesne, C. J., Pujol, R., Lavigne-Rebillard, M., Puel, J. L. and Hamel, C. P. (2002). Downregulation of otospiralin, a novel inner ear protein, causes hair cell degeneration and deafness. *J. Neurosci*. **22**, 1718-1725.

Delprat, B., Ruel, J., Guitton, M. J., Hamard, G., Lenoir, M., Pujol, R., Puel, J. L., Brabet, P. and Hamel, C. P. (2005). Deafness and cochlear fibrocyte alterations in mice deficient for the inner ear protein otospiralin. *Mol. Cell. Biol.* **25**, 847-853.

Erichsen, S., Zuo, J., Curtis, L., Rarey, K. and Hultcrantz, M. (1996). Na,K-ATPase alpha- and beta-isoforms in the developing cochlea of the mouse. *Hear. Res.* **100**, 143-149.

Estevez, R., Boettger, T., Stein, V., Birkenhager, R., Otto, E., Hildebrandt, F. and Jentsch, T. J. (2001). Barttin is a Cl- channel beta-subunit crucial for renal Cl- reabsorption and inner ear K+ secretion. *Nature* **414**, 558-561.
Forge, A. and Wright, T. (2002). The molecular architecture of the inner ear. *Br. Med. Bull.* **63**, 5-24.
Forge, A., Marziano, N. K., Casalotti, S. O., Becker, D. L. and Jagger, D. (2003). The inner ear contains heteromeric channels composed of cx26 and cx30 and deafness-related mutations in cx26 have a dominant negative effect on cx30. *Cell Commun. Adhes.* **10**, 341-346.
Gow, A., Davies, C., Southwood, C. M., Frolenkov, G., Chrustowski, M., Ng, L., Yamauchi, D., Marcus, D. C. and Kachar, B. (2004). Deafness in Claudin 11-null mice reveals the critical contribution of basal cell tight junctions to stria vascularis function. *J. Neurosci.* **24**, 7051-7062.
Henson, M. M. and Henson, O. W., Jr (1988). Tension fibroblasts and the connective tissue matrix of the spiral ligament. *Hear. Res.* **35**, 237-258.
Hequembourg, S. and Liberman, M. C. (2001). Spiral ligament pathology: a major aspect of age-related cochlear degeneration in C57BL/6 mice. *J. Assoc. Res. Otolaryngol.* **2**, 118-129.
Hirose, K. and Liberman, M. C. (2003). Lateral wall histopathology and endocochlear potential in the noise-damaged mouse cochlea. *J. Assoc. Res. Otolaryngol.* **4**, 339-352.
Horiuchi, K., Amizuka, N., Takeshita, S., Takamatsu, H., Katsuura, M., Ozawa, H., Toyama, Y., Bonewald, L. F. and Kudo, A. (1999). Identification and characterization of a novel protein, periostin, with restricted expression to periosteum and periodontal ligament and increased expression by transforming growth factor beta. *J. Bone. Miner. Res.* **14**, 1239-1249.
Ito, M., Spicer, S. S. and Schulte, B. A. (1993). Immunohistochemical localization of brain type glucose transporter in mammalian inner ears: comparison of developmental and adult stages. *Hear. Res.* **71**, 230-238.
Kiernan, A. E., Steel, K. P. and Fekete, D. M. (2002). Development of the mouse inner ear. In *Mouse Development* (ed. J. Rossant and P. Tam), pp. 539-566. San Diego: Academic Press.
Kikuchi, K. and Hilding, D. A. (1966). The development of the stria vascularis in the mouse. *Acta Otolaryngol.* **62**, 277-291.
Kikuchi, T., Adams, J. C., Miyabe, Y., So, E. and Kobayashi, T. (2000). Potassium ion recycling pathway via gap junction systems in the mammalian cochlea and its interruption in hereditary nonsyndromic deafness. *Med. Electron Microsc.* **33**, 51-56.
Kitajiri, S., Miyamoto, T., Mineharu, A., Sonoda, N., Furuse, K., Hata, M., Sasaki, H., Mori, Y., Kubota, T., Ito, J. et al. (2004). Compartmentalization established by claudin-11-based tight junctions in stria vascularis is required for hearing through generation of endocochlear potential. *J. Cell Sci.* **117**, 5087-5096.
Lefebvre, V. and de Crombrugghe, B. (1998). Toward understanding SOX9 function in chondrocyte differentiation. *Matrix Biol.* **16**, 529-540.
Levin, M. (2007). Gap junctional communication in morphogenesis. *Prog. Biophys. Mol. Biol.* **94**, 186-206.
Li, J. and Verkman, A. S. (2001). Impaired hearing in mice lacking aquaporin-4 water channels. *J. Biol. Chem.* **276**, 31233-31237.
Lobe, C. G., Koop, K. E., Kreppner, W., Lomeli, H., Gertsenstein, M. and Nagy, A. (1999). Z/AP, a double reporter for cre-mediated recombination. *Dev. Biol.* **208**, 281-292.
Marcus, D. C., Wu, T., Wangemann, P. and Kofuji, P. (2002). KCNJ10 (Kir4.1) potassium channel knockout abolishes endocochlear potential. *Am. J. Physiol. Cell Physiol.* **282**, C403-C407.
Minowa, O., Ikeda, K., Sugitani, Y., Oshima, T., Nakai, S., Katori, Y., Suzuki, M., Furukawa, M., Kawase, T., Zheng, Y. et al. (1999). Altered cochlear fibrocytes in a mouse model of DFN3 nonsyndromic deafness. *Science* **285**, 1408-1411.
Moorman, A. F., Houweling, A. C., de Boer, P. A. and Christoffels, V. M. (2001). Sensitive nonradioactive detection of mRNA in tissue sections: novel application of the whole-mount in situ hybridization protocol. *J. Histochem. Cytochem.* **49**, 1-8.
Naiche, L. A., Harrelson, Z., Kelly, R. G. and Papaioannou, V. E. (2005). T-box genes in vertebrate development. *Annu. Rev. Genet.* **39**, 219-239.
Phippard, D., Heydemann, A., Lechner, M., Lu, L., Lee, D., Kyin, T. and Crenshaw, E.B., 3rd (1998). Changes in the subcellular localization of the Brn4 gene product precede mesenchymal remodeling of the otic capsule. *Hear. Res.* **120**, 77-85.
Phippard, D., Lu, L., Lee, D., Saunders, J. C. and Crenshaw, E. B., 3rd (1999). Targeted mutagenesis of the POU-domain gene Brn4/Pou3f4 causes developmental defects in the inner ear. *J. Neurosci.* **19**, 5980-5989.
Raphael, Y. and Altschuler, R. A. (2003). Structure and innervation of the cochlea. *Brain Res. Bull.* **60**, 397-422.
Sadanaga, M. and Morimitsu, T. (1995). Development of endocochlear potential and its negative component in mouse cochlea. *Hear. Res.* **89**, 155-161.
Sagara, T., Furukawa, H., Makishima, K. and Fujimoto, S. (1995). Differentiation of the rat stria vascularis. *Hear. Res.* **83**, 121-132.
Spicer, S. S. and Schulte, B. A. (1991). Differentiation of inner ear fibrocytes according to their ion transport related activity. *Hear. Res.* **56**, 53-64.
Steel, K. P., Davidson, D. R. and Jackson, I. J. (1992). TRP-2/DT, a new early melanoblast marker, shows that steel growth factor (c-kit ligand) is a survival factor. *Development* **115**, 1111-1119.
Teubner, B., Michel, V., Pesch, J., Lautermann, J., Cohen-Salmon, M., Söhl, G., Janhke, K., Winterhager, E., Heberhold, C., Hardelin, J. et al. (2003). Connexin30 (GjB6)-deficiency causes severe hearing impairment and lack of endocochlear potential. *Hum. Mol. Genet.* **12**, 13-21.
Thiery, J. P. and Sleeman, J. P. (2006). Complex networks orchestrate epithelial-mesenchymal transitions. *Nat. Rev. Mol. Cell. Biol.* **7**, 131-142.
Vanderburg, C. R. and Hay, E. D. (1996). E-cadherin transforms embryonic corneal fibroblasts to stratified epithelium with desmosomes. *Acta Anat. (Basel)* **157**, 87-104.
Vestweber, D. and Kemler, R. (1984). Some structural and functional aspects of the cell adhesion molecule uvomorulin. *Cell Diff.* **15**, 269-273.
Vetter, D. E., Mann, J. R., Wangemann, P., Liu, J., McLaughlin, K. J., Lesage, F., Marcus, D. C., Lazdunski, M., Heinemann, S. F. and Barhanin, J. (1996). Inner ear defects induced by null mutation of the isk gene. *Neuron* **17**, 1251-1264.
Wangemann, P. (2002). K+ cycling and the endocochlear potential. *Hear. Res.* **165**, 1-9.
Xia, A., Kikuchi, T., Hozawa, K., Katori, Y. and Takasaka, T. (1999). Expression of connexin 26 and Na,K-ATPase in the developing mouse cochlear lateral wall: functional implications. *Brain Res.* **846**, 106-111.
Yamasaki, M., Komune, S., Shimozono, M., Matsuda, K. and Haruta, A. (2000). Development of monovalent ions in the endolymph in mouse cochlea. *ORL. J. Otorhinolaryngol. Relat. Spec.* **62**, 241-246.